



## Theoretical study of molecular-frame angular emission distributions of electrons emitted by interatomic Coulombic decay from helium dimers

Abir Mhamdi <sup>1</sup>, Jonas Rist,<sup>2</sup> Tilo Havermeier,<sup>2</sup> Reinhard Dörner,<sup>2</sup> Till Jahnke,<sup>2</sup> and Philipp V. Demekhin <sup>1,\*</sup>

<sup>1</sup>*Institut für Physik und CINSaT, Universität Kassel, Heinrich-Plett-Strasse 40, D-34132 Kassel, Germany*

<sup>2</sup>*Institut für Kernphysik, J. W. Goethe-Universität, Max-von-Laue-Strasse 1, D-60438 Frankfurt am Main, Germany*



(Received 22 October 2019; accepted 23 January 2020; published 10 February 2020)

Molecular frame angular distributions of electrons released by interatomic Coulombic decay of  $\text{He}^{+*}(2\ell)\text{-He}$  states are studied theoretically by means of electronic structure and nonadiabatic nuclear dynamics calculations. In previous experimental work [*Phys. Rev. A* **82**, 063405 (2010)], distinct variations of the angular emission patterns have been observed for different ranges of kinetic-energy release of the fragment ions. Good agreement between the presently computed and these measured angular distributions can be achieved by assuming nonequal populations of  $^2\Sigma_{g/u}^+$  and  $^2\Pi_{g/u}$  decaying electronic states via initial shake-up ionization of the dimers.

DOI: [10.1103/PhysRevA.101.023404](https://doi.org/10.1103/PhysRevA.101.023404)

### I. INTRODUCTION

Since its theoretical prediction in 1997 [1] and subsequent experimental verification [2,3], interatomic Coulombic decay (ICD) has become a well-established field of research, involving many scientific groups all over the world (for review articles see, e.g., Refs. [4–7]). By ICD, a (typically) low-energy electron [8–10] is emitted from a loosely bound compound of atoms or molecules via a nonlocal electronic relaxation. When emerging from the ion, these slow electrons accumulate detailed information on the electronic structure of the decaying system and on the dynamics of the decay. The most complete information is imprinted in the angular emission distributions of the emitted electrons in the molecular frame of reference [11–14], i.e., in so-called molecular frame angular distributions (MFADs). At present, MFADs of such ICD electrons emitted by different types of ICD processes have been studied employing neon dimers [15–18], HeNe [19], and helium dimers [20].

ICD, in helium dimers, which is the topic of the present theoretical paper, was discovered almost ten years ago.  $\text{He}_2$  is the most weakly bound noble gas van der Waals system with a binding energy of only about 150 neV [21] and a mean bond length of about 52 Å [22]. In Refs. [23,24], it was observed experimentally that excited states of  $\text{He}_2^{+*}$  are able to transfer about 40 eV of electronic excitation energy from one helium atom to its neighbor via ICD. In the process, an excited  $n\ell(n \geq 2)$  electron on the ionized site  $\text{He}^{+*}$  of the dimer relaxes to the  $\text{He}^+(1s)$  ground ionic state. The released energy is used to ionize the neighboring neutral site, producing doubly ionized final states ( $\text{He}^+\text{-He}^+$ ) and the ICD electron. This ultra-long-range energy transfer by ICD occurring in He dimers has been interpreted by *ab initio* calculations in Refs. [25,26], which uncovered the

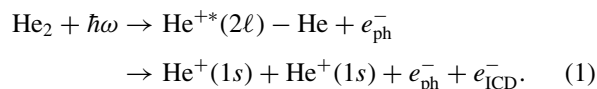
utmost important role of the nuclear motion accompanying this decay [27].

Several fundamental aspects of the ICD in He dimers, such as its temporal evolution [28], recapture of photoelectrons induced by ICD [29], and MFADs of ICD electrons [20], were reported in the literature, so far. In the latter work, a pronounced variation of the MFAD for different regions of the kinetic-energy release (KER) of the ions was observed experimentally. This strong dependence of the MFAD on the internuclear distance at which the decay takes place was qualitatively explained by a very simple model implying a coherent superposition of two spherical electron waves emitted by virtual photon exchange between the two helium atoms. The respective individual MFADs obtained for the transitions between all initial and final electronic states were obtained by taking the symmetry of the involved states into account and weighting them with the respective probabilities taken from the theoretical KER spectrum.

In the present paper, we investigate MFADs of ICD electrons in  $\text{He}_2$  employing a full theoretical modeling and provide an interpretation of the experimental results from Ref. [20]. For this purpose, we utilize the previously developed theoretical approach, which was recently applied to study ICD in  $\text{Ne}_2$  [18] and HeNe [19]. This approach is outlined in Sec. II. The theoretical results are reported and discussed in Sec. III. We conclude in Sec. IV with a brief summary and outlook.

### II. THEORY

The process relevant to the present paper can schematically be represented as follows:



In the first step, a photon with an energy of  $\hbar\omega = 68.86$  eV [20] ionizes one of the helium atoms and simultaneously

\*demekhin@physik.uni-kassel.de

excites its remaining  $1s$  electron to one of the  $2s$  or  $2p$  states. This step populates the following eight symmetry-adapted electronic states of the dimer:  $2\sigma_{g/u}(2s_0)^2\Sigma_{g/u}^+$ ,  $3\sigma_{g/u}(2p_0)^2\Sigma_{g/u}^+$ , and  $1\pi_{g/u}(2p_{\pm 1})^2\Pi_{g/u}$ . In the second step, the excited ion of the dimer deexcites, and the excess energy is used to release a slow ICD electron from the neighboring neutral helium atom. This generates a dication in one of its lowermost repulsive electronic states:  $^1\Sigma_g^+$  or  $^3\Sigma_u^+$ . The remaining part of the excess energy is shared between the KER of the two ionic fragments and the kinetic energy of the ICD electron.

The nuclear dynamics accompanying the ICD process (1) can be described in terms of vibronic eigenstates [30] of the ground neutral singly ionized, additionally excited initial decaying, and doubly ionized final states of the dimer. The amplitude for the emission of a partial electron wave [31] of energy  $\varepsilon_{\text{ICD}}$  with angular momentum quantum numbers  $L, M$  (given in the frame of the dimer) via the decay transition from the initial electronic state  $|I\rangle$  into the nuclear continuum state  $|v_f\rangle$  with energy  $\varepsilon_{v_f}$  ( $=\text{KER}$ ) of the final electronic state of the “ion + ICD electron”  $|F\rangle$  is given by [25]

$$A_{FI}^{LM}(\varepsilon_{\text{ICD}}, \varepsilon_{v_f}) = \sum_{v_i} \frac{\langle v_f | W_{FI}^{LM} | v_i \rangle \langle v_i | D_I | 0 \rangle}{\varepsilon_{\text{ICD}} + \varepsilon_{v_f} - E_{v_i} + i\Gamma_{v_i}/2}. \quad (2)$$

Here,  $|0\rangle$  is the ground vibrational state of the neutral dimer,  $D_I$  is the electronic transition matrix element for the shake-up ionization of the dimer in the first step of the process (1), and  $W_{FI}^{LM}$  is the respective ICD transition matrix element. We note that Eq. (2) describes the nuclear dynamics accompanying ICD only approximately. This is because it ignores rotational excitation by photoelectron recoil, which, for  $\text{He}_2$ , may have significant influence.

The summation in Eq. (2) must be performed over all decaying vibronic eigenstates  $|v_i\rangle$  with energy  $E_{v_i}$  and total decay width  $\Gamma_{v_i}$ , which are solutions of the local non-Hermitian nuclear Hamiltonian  $\hat{T}_R + V_I(R) - i\Gamma_I(R)/2$  [32]. Here,  $\hat{T}_R$  is the kinetic-energy operator,  $V_I(R)$  is the respective potential-energy curve, and  $\Gamma_I(R)$  is the total decay width of initial state  $|I\rangle$ , which includes its relaxation via ICD as well as by the competing radiative decay [25]. In addition, the respective nuclear dynamics is essentially nonadiabatic [25]. This one-dimensional nuclear vibrational motion was described here by the theoretical approach of Refs. [33,34], which includes the underlying nonadiabatic effects in the decaying states. The relevant diabatic potential-energy curves and nonadiabatic couplings were taken from Refs. [25,26].

The partial MFADs for the individual  $|F\rangle \leftarrow |I\rangle$  transition with given KER and ICD electron energy is defined through the respective partial amplitudes (2) as follows:

$$\frac{d\sigma_{FI}}{d\Omega}(\varepsilon_{\text{ICD}}, \varepsilon_{v_f}) = \left| \sum_{L,M} (-i)^L A_{FI}^{LM}(\varepsilon_{\text{ICD}}, \varepsilon_{v_f}) Y_{LM}(\theta, \varphi) \right|^2. \quad (3)$$

Here, the emission angles of the ICD electron  $\theta, \varphi$  are defined in the dimer frame. The partial MFADs representing a given KER value  $\varepsilon_{v_f}$  are obtained by integrating the MFADs (3)

over the ICD electron energy  $\varepsilon_{\text{ICD}}$ ,

$$\frac{d\sigma_{FI}}{d\Omega}(\varepsilon_{v_f}) = \int \frac{d\sigma_{FI}}{d\Omega}(\varepsilon_{\text{ICD}}, \varepsilon_{v_f}) d\varepsilon_{\text{ICD}}. \quad (4)$$

Finally, the total MFAD of ICD electrons belonging to a given KER value is the sum of partial MFADs over all initial and final electronic states of the decay. Additional integration over all values of KER yields the total MFAD of all ICD electrons which are different by symmetry. Alternatively, additional integration over all emission angles yields the total KER spectrum.

The electronic decay transition amplitudes  $W_{FI}^{LM}$  entering Eq. (2), were computed using the single center (SC) method and code [35,36], which allows for an accurate description of excitation [33,37–39] and angle-resolved ionization of diatomic molecules [40–43] and even weakly bound dimers [18,19,44]. The wave functions of excited and ionized electrons of the helium dimer were computed within the frozen-core Hartree-Fock approximation. The center of the dimer was chosen in the middle of the two helium atoms. The SC expansions of occupied orbitals of the dimer included angular momenta with  $\ell_c \leq 99$ , whereas the expansions of the excited or ionized electrons were restricted to partial harmonics with  $\ell_\varepsilon \leq 49$ . The SC calculations were performed at different internuclear distances. Thereby, the partial amplitudes (2) were computed beyond the Franck-Condon approximation, which is essential for description of ICD processes.

The computation of the ICD transition amplitudes  $W_{FI}^{LM}$  in homonuclear dimers is an intricate task [45,46]. This is because involved electronic states are delocalized due to inversion symmetry. As a consequence, single-configuration descriptions of the initial and final states of the decay lead to incorrect transition rates, which, in addition to the desired interatomic contribution, incorporate that from intra-atomic processes [45,46]. Therefore, three-electron wave functions of the initial and final states of ICD in helium dimers need a proper constriction. In order to exclude energetically forbidden intra-atomic processes, here, we represent the three-electron symmetry-adapted initial states of the decay in terms of localized one-particle orbitals. For the positive projection of the total spin, the respective doublet states, which can relax by ICD, read

$$|I_{G/U}\rangle = \frac{1}{\sqrt{2}}(|1s_L^2 2\ell_R^+ \pm |1s_R^2 2\ell_L^+ \rangle). \quad (5)$$

To further represent these initial states in terms of symmetry-adapted one-particle orbitals, straightforward transformations  $|L/R\rangle = \frac{1}{\sqrt{2}}(|g\rangle \pm |u\rangle)$  need to be performed for each localized one-particle orbital according to its local symmetry (not shown for brevity).

In order to properly design the three-electron symmetry-adapted final states of the decay, one first needs to construct electronic states of the dication which represent open ICD channels. These are the two lowermost singlet and triplet dicationic states in which two remaining  $1s$  electrons are localized on different atomic sides. This can also be performed by starting from the localized one-particle basis with subsequent transformation to the symmetry-adapted basis (not shown for brevity). In the second step, the three-electron final ICD states of the ion + ICD electron need to be constructed. For the

positive projection of the total spin, the respective doublet continuum states, representing two lowermost  $^1\Sigma_g^+$  and  $^3\Sigma_u^+$  electronic states of the doubly charged ion, read

$$\begin{aligned} |F\rangle &= ({}^1\Sigma_g^+) \varepsilon \lambda_{g/u}^+ {}^2\Lambda_{g/u} \rangle \\ &= \frac{1}{\sqrt{2}} (|1s_g^2 \varepsilon \lambda_{g/u}^+ \rangle - |1s_u^2 \varepsilon \lambda_{g/u}^+ \rangle), \end{aligned} \quad (6a)$$

$$\begin{aligned} |F\rangle &= ({}^3\Sigma_u^+) \varepsilon \lambda_{g/u}^+ {}^2\Lambda_{u/g} \rangle \\ &= \frac{1}{\sqrt{6}} (|1s_g^+ 1s_u^- \varepsilon \lambda_{g/u}^+ \rangle + |1s_g^- 1s_u^+ \varepsilon \lambda_{g/u}^+ \rangle - 2|1s_g^+ 1s_u^+ \varepsilon \lambda_{g/u}^- \rangle). \end{aligned} \quad (6b)$$

### III. RESULTS AND DISCUSSION

Accurate calculation of electronic transition amplitudes for the ionization and simultaneous excitation (i.e., for the shake-up ionization) of molecules is a cumbersome task. Therefore, as proposed in previous theoretical studies of ICD in He<sub>2</sub> [20,25], we first assume an equal populations of all initial ICD states  $|I\rangle$  by shake-up ionization of one of the atoms of the dimer. Thereby the population transition amplitude  $\langle v_f | D_I | 0 \rangle$  in Eq. (2) can be replaced by the respective Franck-Condon factor  $\langle v_f | 0 \rangle$ . Results of these calculations are depicted in Figs. 1(a) and 2(a). Figure 1(a) illustrates good agreement between the computed and the measured [24] total KER spectra (cf., positions of maxima and their strengths for the red solid curve and open circles). On the contrary, the computed total MFAD of the ICD electrons shown in Fig. 2(a) is very different from the measured one reported in Ref. [20] (positions of the maxima and minima of the red solid curve and open circles are even swapped). Moreover, the calculations employing an equal population of initial states fail to reproduce the partial MFADs of ICD electrons reported in Ref. [20] for different ranges of KERs (not shown here for brevity).

In the experiment [20], the shake-up ionization of helium dimers at a photon energy of 68.86 eV releases photoelectrons  $e_{\text{ph}}^-$  with relatively small kinetic energy of about 3.5 eV. It is well known that the probabilities for shake-up ionization of helium atoms to produce  $2p$  and  $2s$  excited states are not equal, i.e., close to the ionization threshold, a ratio of the respective cross sections deviates from the statistical value of 3 [47–49]. For helium dimers, one can assume that the cross sections for the population of  $2p_0$  and  $2p_{\pm 1}$  excited states are nonequal, as well, i.e., do not scale as one to two for the respective  $\sigma$  and  $\pi$  states. Moreover, the probabilities to populate *gerade* and *ungerade* excited states  $2\sigma_{g/u}(2s_0)$ ,  $3\sigma_{g/u}(2p_0)$ , and  $1\pi_{g/u}(2p_{\pm 1})$  of the dimer may also differ.

In order to understand the disagreement between the computed and the measured [20] ICD electron MFADs in Fig. 2(a), we took a closer look at the total MFADs computed for the individual decaying electronic states of the dimer depicted in Fig. 3. As one can see from Fig. 3(b), an enhancement of the contribution from the  $3\sigma_g$  state (the red solid curve) can improve the agreement between the theory and the experiment at emission angles of 90° and 270°. An additional reduction of the emission probability at emission directions

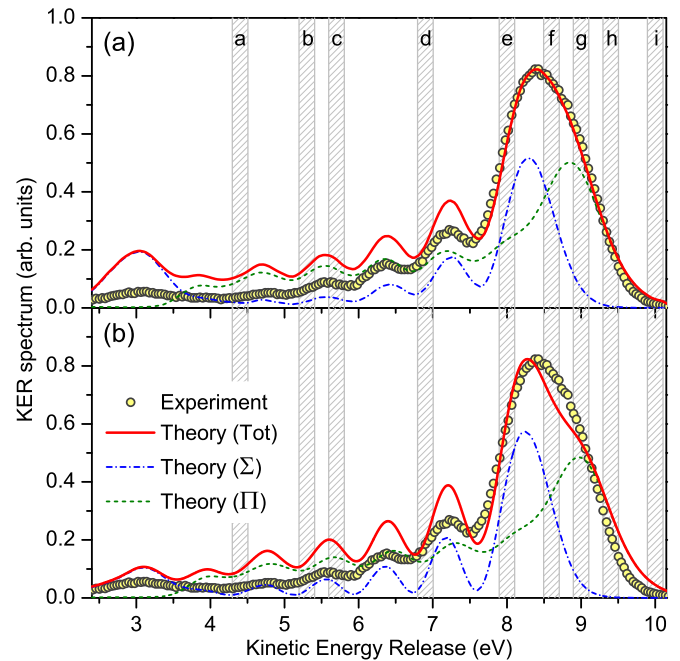


FIG. 1. Measured kinetic-energy release spectrum [24] (the open circles) together with the partial and total (see the legend) KER spectra computed in the present paper within different approximations. The experimental uncertainties are smaller than the size of the circles. Panel (a): results of the calculation implying equal populations of the decaying electronic states via initial shake-up ionization of helium dimers. Panel (b): results of the model calculations assuming nonequal populations of the decaying states (see the text for details). The shaded vertical stripes indicate KER regions for which MFADs of the ICD electrons are depicted in Fig. 4 (the lowercase letters on the top correspond to the panels of Fig. 4).

of 0° and 180° can be achieved by suppressing the individual contributions from the  $2\sigma_{g/u}$  and  $3\sigma_u$  states. Moreover, since ICD of the  $2\sigma_{g/u}$  states contributes mainly to the formation of the low-energy part of the KER spectrum [25], suppressing their contributions will also yield an improved agreement between the computed and the measured KER spectra in Fig. 1(a).

Starting with these assumptions, we found a set of populations of the initial decaying states which brings the computed total MFAD of ICD electrons in a reasonable agreement with the experiment [20] [see Fig. 2(b)]. In particular, by keeping the populations of the  $1\pi_{g/u}$  states to be 1.0, as a reference, we increased the population of the  $3\sigma_g$  state to 1.5 and decreased the populations of the  $2\sigma_{g/u}$  and  $3\sigma_u$  states to 0.4. We note that results of such calculations are rather robust to a variation of these parameters within the range of about  $\pm 10\%$ . As expected, introducing this set of populations improves the agreement between the computed and the measured low-energy KER spectrum [cf., the red solid curve and open circles in Fig. 1(b)]. However, it slightly reduces the agreement on the high-energy side [note a small shoulder in the computed KER at about 9 eV in Fig. 1(b)]. More importantly, this model allows reproducing the experimental partial MFADs of ICD electrons reported in Ref. [20] for the different values of KER (see Fig. 4).

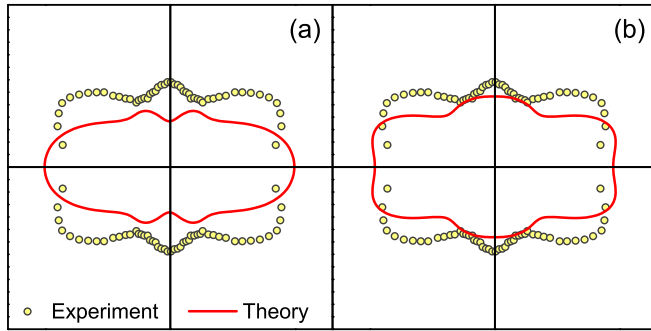


FIG. 2. Measured angular distributions of ICD electrons [20] and computed in the present paper within different approximations. The distributions were obtained integrating over all kinetic-energy releases. The experimental uncertainties are smaller than the size of the circles. The dimer is oriented horizontally. Panel (a): results of the calculation implying equal populations of the decaying electronic states via initial shake-up ionization of helium dimers. Panel (b): results of the model calculations assuming nonequal populations of the decaying states (see the text for details).

A closer inspection of Fig. 4 (together with the individual MFADs from Fig. 3) connects the strong variation of the MFAD of ICD electrons for different kinetic energies of the ions directly to the involved states. In particular, emission distributions depicted in Figs. 4(a)–4(c) (the uppermost row) are mainly produced by the decay of the  $1\pi_{g/u}$  states. A somewhat increased emission probability in the  $0^\circ/180^\circ$  directions in Fig. 4(a) indicates a notable contribution from the  $2\sigma_{g/u}$  and  $3\sigma_{g/u}$  states. The distributions in Figs. 4(d)–4(f) (the middle row) are produced by a dominant contribution from the  $3\sigma_{g/u}$  states, with a notable contribution from the  $1\pi_{g/u}$  states in Fig. 4(d). For the lowermost row of Figs. 4(g)–4(i), ICD of the  $1\pi_{g/u}$  states plays again a dominant role. These conclusions are fully confirmed by the relative contributions of all  $\Sigma$  and all  $\Pi$  states to the total KER spectrum depicted in Fig. 1(b) by the blue dashed-dotted and green dashed curves, respectively. As one can see from Fig. 1(b), the contribution from all  $\Sigma$  states is particularly relevant only for the middle range of KER spectrum from about 5.9 to 8.8 eV (see the three shaded vertical stripes in the middle labeled by lowercase letters d–f).

The populations of the initial decaying states of helium dimers, which allowed us to interpret previous measurements,

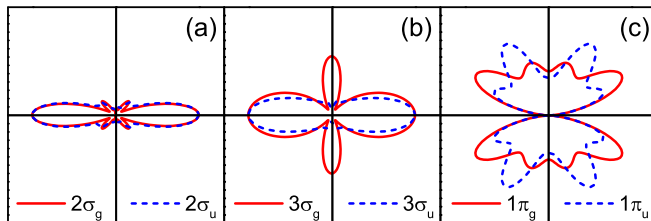


FIG. 3. Total angular distributions of ICD electrons (i.e., integrated over all values of KER) computed in the present paper for all individual decaying states (see the legend in each panel). The dimer is oriented horizontally, and the individual MFADs are normalized to their maxima.

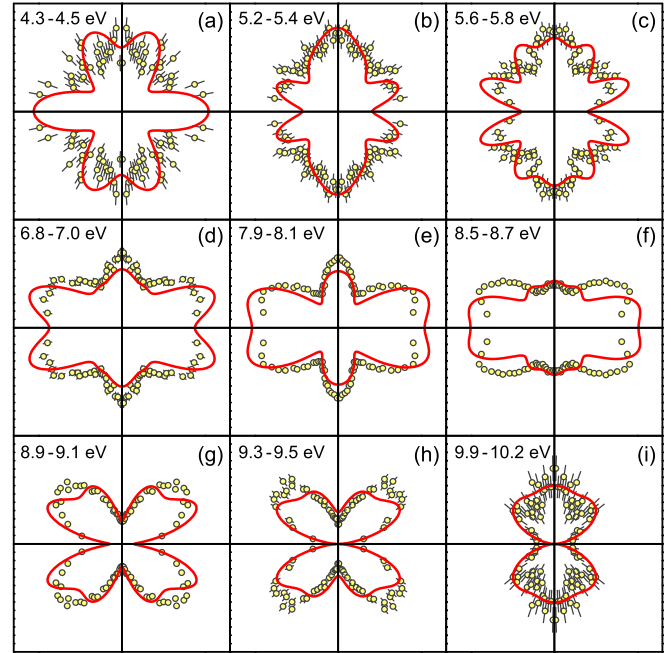


FIG. 4. Measured ICD electron MFADs [20] and MFADs computed in the present paper for different regions of KER (as indicated in each panel and by the vertical shaded stripes in Fig. 1). The theory implies nonequal populations of the decaying electronic states via the initial shake-up ionization of helium dimers [these data correspond to Figs. 1(b) and 2(b)]. The dimer is oriented horizontally, and the individual MFADs are shown on relative scales.

deviate from the equal populations, expected for helium atoms from statistical reasons, by about  $\pm 50\%$ . References [47–49] report deviations of the ratio of probabilities for the shake-up ionization of helium atom to produce  $2p$  and  $2s$  excited states from its statistical value of 3 on a very similar scale (see Fig. 5 in Ref. [49] which reports a compilation of different experimental and theoretical data from the literature). A semiquantitative analysis of the experimental photoelectron angular distributions, performed by one of us, also suggests that, in helium dimers, populations of the initial decaying states can differ considerably (see Chap. 5.1.2 of Ref. [50]). A quantitative clarification of this issue is a very formidable task, which is outside the scope of the present paper. It is, therefore, left for future studies of ICD in helium dimers. Such studies, however, ought to be performed on an improved level of theory, which includes the electron correlations in the photoionization step and accounts for the recoil-induced rovibrational motion of the dimer neglected in the present paper.

#### IV. CONCLUSION

ICD in helium dimers has been studied theoretically using a previously developed theoretical approach. The respective transition amplitudes are computed by means of the single center method and include nonadiabatic nuclear dynamics accompanying the decay. The accurate electronic decay transition amplitudes for the emission of partial electron waves allowed us to access the angular emission distributions

of ICD electrons. The present calculations, implying equal populations of the decaying electronic states by the shake-up ionization of the dimer, reproduce the previously measured KER spectrum but fail to explain the earlier observed partial and total MFADs of the ICD electrons. In order to explain this discrepancy, we assume nonequal populations of the initial decaying states by the shake-up ionization. A careful inspection of the presently computed KER spectra and MFADs of ICD electrons for individual decaying states enabled us to find a set of initial populations which yields good agreement between the computed and the measured total MFAD of ICD electrons. Simultaneously, this set of initial populations improves the agreement between the computed and the measured low-energy KER spectra and allows to reproduce and explain the strong variation of the partial MFADs measured for different KER values.

Our study confirms that the rich structure observed in the KER spectrum is mainly determined by the nuclear dynamics, and electronic properties of the process play only a moderate role. On the contrary, as expected, the strong variation of the MFAD of ICD electrons as a function of KER is provided by electronic properties of the process with only a moderate

role of the nuclear dynamics. The present theoretical results suggest that individual populations of the initial decaying states via the shake-up ionization of helium dimers can substantially vary with photon energy (photoelectron kinetic energy), especially in a close proximity to the ionization threshold. This conclusion is particularly relevant for the so-called postcollision interaction streaking [28] techniques, which rely on extremely low energy of photoelectrons. Owing to very different initial populations of the decaying states at very low photoelectron kinetic energies, one would expect completely different total and partial MFADs of ICD electrons in helium dimers as compared to those presented here and in Ref. [20].

#### ACKNOWLEDGMENTS

This work was supported by the Deutsche Forschungsgemeinschaft within the DFG Research Unit FOR 1789 “Interatomic and Intermolecular Coulombic Decay.” We are grateful to N. Sisourat and N. Kryzhevoi for providing us with potential-energy curves and nonadiabatic couplings of helium dimers and for many valuable discussions.

- 
- [1] L. S. Cederbaum, J. Zobeley, and F. Tarantelli, *Phys. Rev. Lett.* **79**, 4778 (1997).
- [2] S. Marburger, O. Kugeler, U. Hergenbahn, and T. Möller, *Phys. Rev. Lett.* **90**, 203401 (2003).
- [3] T. Jahnke, A. Czasch, M. S. Schöffler, S. Schössler, A. Knapp, M. Kász, J. Titze, C. Wimmer, K. Kreidi, R. E. Grisenti, A. Staudte, O. Jagutzki, U. Hergenbahn, H. Schmidt-Böcking, and R. Dörner, *Phys. Rev. Lett.* **93**, 163401 (2004).
- [4] V. Averbukh, Ph. V. Demekhin, P. Kolorenč, S. Scheit, S. D. Stoychev, A. I. Kuleff, Y.-C. Chiang, K. Gokhberg, S. Kopelke, N. Sisourat, and L. S. Cederbaum, *J. Electron. Spectrosc. Relat. Phenom.* **183**, 36 (2011).
- [5] U. Hergenbahn, *J. Electron. Spectrosc. Relat. Phenom.* **184**, 78 (2011).
- [6] U. Hergenbahn, *Int. J. Radiat. Biology* **88**, 871 (2012).
- [7] T. Jahnke, *J. Phys. B: At., Mol. Opt. Phys.* **48**, 082001 (2015).
- [8] M. Mucke, M. Braune, S. Barth, M. Furstel, T. Lischke, V. Ulrich, T. Arion, A. M. Bradshaw, U. Becker, and U. Hergenbahn, *Nat. Phys.* **6**, 143 (2010).
- [9] T. Jahnke, H. Sann, T. Havermeier, K. Kreidi, C. Stuck, M. Meckel, M. Schöffler, N. Neumann, R. Wallauer, S. Voss *et al.*, *Nat. Phys.* **6**, 139 (2010).
- [10] F. Trinter, M. S. Schöffler, H.-K. Kim, F. P. Sturm, K. Cole, N. Neumann, A. Vredenburg, J. Williams, I. Bocharova, R. Guillemin *et al.*, *Nature (London)* **505**, 664 (2014).
- [11] A. Landers, T. Weber, I. Ali, A. Cassimi, M. Hattass, O. Jagutzki, A. Nauert, T. Osipov, A. Staudte, M. H. Prior, H. Schmist-Böcking, C. L. Cocke, and R. Dörner *Phys. Rev. Lett.* **87**, 013002 (2001).
- [12] T. Jahnke, Th. Weber, A. L. Landers, A. Knapp, S. Schössler, J. Nickles, S. Kammer, O. Jagutzki, L. Schmidt, A. Czasch *et al.*, *Phys. Rev. Lett.* **88**, 073002 (2002).
- [13] J. B. Williams, C. S. Trevisan, M. S. Schöffler, T. Jahnke, I. Bocharova, H. Kim, B. Ulrich, R. Wallauer, F. Sturm, T. N. Rescigno, A. Belkacem, R. Dörner, T. Weber, C. W. McCurdy, and A. L. Landers, *Phys. Rev. Lett.* **108**, 233002 (2012).
- [14] H. Fukuzawa, R. R. Lucchese, X.-J. Liu, K. Sakai, H. Iwayama, K. Nagaya, K. Kreidi, M. S. Schöffler, J. R. Harries, Y. Tamenori *et al.*, *J. Chem. Phys.* **150**, 174306 (2019).
- [15] T. Jahnke, A. Czasch, M. S. Schöffler, S. Schössler, M. Kász, J. Titze, K. Kreidi, R. E. Grisenti, A. Staudte, O. Jagutzki *et al.*, *J. Phys. B: At., Mol. Opt. Phys.* **40**, 2597 (2007).
- [16] K. Kreidi, T. Jahnke, Th. Weber, T. Havermeier, R. E. Grisenti, X. Liu, Y. Morisita, S. Schössler, L. Ph. H. Schmidt, M. S. Schöffler *et al.*, *J. Phys. B: At., Mol. Opt. Phys.* **41**, 101002 (2008).
- [17] S. K. Semenov, K. Kreidi, T. Jahnke, Th. Weber, T. Havermeier, R. E. Grisenti, X. Liu, Y. Morisita, L. Ph. H. Schmidt, M. S. Schöffler *et al.*, *Phys. Rev. A* **85**, 043421 (2012).
- [18] A. Mhamdi, J. Rist, D. Aslitürk, M. Weller, N. Melzer, D. Trabert, M. Kircher, I. Vela-Pérez, J. Siebert, S. Eckart *et al.*, *Phys. Rev. Lett.* **121**, 243002 (2018).
- [19] A. Mhamdi, F. Trinter, C. Rauch, M. Weller, J. Rist, M. Waitz, J. Siebert, D. Metz, C. Janke, G. Kastirke *et al.*, *Phys. Rev. A* **97**, 053407 (2018).
- [20] T. Havermeier, K. Kreidi, R. Wallauer, S. Voss, M. Schöffler, S. Schössler, L. Foucar, N. Neumann, J. Titze, H. Sann *et al.*, *Phys. Rev. A* **82**, 063405 (2010).
- [21] S. Zeller, M. Kunitski, J. Voigtsberger, A. Kalinin, A. Schottelius, C. Schober, M. Waitz, H. Sann, A. Hartung, T. Bauer *et al.*, *Proc. Natl. Acad. Sci. USA* **113**, 14651 (2016).
- [22] R. E. Grisenti, W. Schöllkopf, J. P. Toennies, G. C. Hegerfeldt, T. Köhler, and M. Stoll, *Phys. Rev. Lett.* **85**, 2284 (2000).
- [23] N. Sisourat, N. V. Kryzhevoi, P. Kolorenč, S. Scheit, T. Jahnke, and L. S. Cederbaum, *Nat. Phys.* **6**, 508 (2010).

- [24] T. Havermeier, T. Jahnke, K. Kreidi, R. Wallauer, S. Voss, M. Schöffler, S. Schössler, L. Foucar, N. Neumann, J. Titze *et al.*, *Phys. Rev. Lett.* **104**, 133401 (2010).
- [25] N. Sisourat, N. V. Kryzhevoi, P. Kolorenč, S. Scheit, and L. S. Cederbaum, *Phys. Rev. A* **82**, 053401 (2010).
- [26] P. Kolorenč, N. V. Kryzhevoi, N. Sisourat, and L. S. Cederbaum, *Phys. Rev. A* **82**, 013422 (2010).
- [27] N. Sisourat, H. Sann, N. V. Kryzhevoi, P. Kolorenč, T. Havermeier, F. Sturm, T. Jahnke, H.-K. Kim, R. Dörner, and L. S. Cederbaum, *Phys. Rev. Lett.* **105**, 173401 (2010).
- [28] F. Trinter, J. B. Williams, M. Weller, M. Waitz, M. Pitzer, J. Voigtsberger, C. Schober, G. Kastirke, C. Müller, C. Gohl *et al.*, *Phys. Rev. Lett.* **111**, 093401 (2013).
- [29] P. Burzynski, F. Trinter, J. B. Williams, M. Weller, M. Waitz, M. Pitzer, J. Voigtsberger, C. Schober, G. Kastirke, C. Müller *et al.*, *Phys. Rev. A* **90**, 022515 (2014).
- [30] N. Moiseyev, S. Scheit, and L. S. Cederbaum, *J. Chem. Phys.* **121**, 722 (2004).
- [31] N. A. Cherepkov, *J. Phys. B: At. Mol. Phys.* **14**, 2165 (1981).
- [32] L. S. Cederbaum and W. Domcke, *J. Phys. B: At. Mol. Phys.* **14**, 4665 (1981).
- [33] P. V. Demekhin, D. V. Omel'yanenko, B. M. Lagutin, V. L. Sukhorukov, L. Werner, A. Ehresmann, K.-H. Schartner, and H. Schmoranzner, *Opt. Spektrosk.* **102**, 318 (2007).
- [34] F. V. Demekhin, D. V. Omel'yanenko, B. M. Lagutin, V. L. Sukhorukov, L. Werner, A. Ehresmann, K.-H. Schartner, and H. Schmoranzner, *Russ. J. Phys. Chem. B* **1**, 213 (2007).
- [35] P. V. Demekhin, A. Ehresmann, and V. L. Sukhorukov, *J. Chem. Phys.* **134**, 024113 (2011).
- [36] S. A. Galitskiy, A. N. Artemyev, K. Jänkälä, B. M. Lagutin, and P. V. Demekhin, *J. Chem. Phys.* **142**, 034306 (2015).
- [37] A. Ehresmann, L. Werner, S. Klumpp, H. Schmoranzner, P. V. Demekhin, B. M. Lagutin, V. L. Sukhorukov, S. Mickat, S. Kammer, B. Zimmermann, and K.-H. Schartner, *J. Phys. B: At., Mol. Opt. Phys.* **37**, 4405 (2004).
- [38] A. Ehresmann, P. V. Demekhin, W. Kielich, I. Haar, M. A. Schlüter, V. L. Sukhorukov, and H. Schmoranzner, *J. Phys. B: At., Mol. Opt. Phys.* **42**, 165103 (2009).
- [39] P. V. Demekhin, V. L. Sukhorukov, H. Schmoranzner, and A. Ehresmann, *J. Chem. Phys.* **132**, 204303 (2010).
- [40] P. V. Demekhin, I. D. Petrov, V. L. Sukhorukov, W. Kielich, P. Reiss, R. Hentges, I. Haar, H. Schmoranzner, and A. Ehresmann, *Phys. Rev. A* **80**, 063425 (2009); **81**, 069902(E) (2010).
- [41] P. V. Demekhin, I. D. Petrov, T. Tanaka, M. Hoshino, H. Tanaka, K. Ueda, W. Kielich, and A. Ehresmann, *J. Phys. B: At., Mol. Opt. Phys.* **43**, 065102 (2010).
- [42] P. V. Demekhin, I. D. Petrov, V. L. Sukhorukov, W. Kielich, A. Knie, H. Schmoranzner, and A. Ehresmann, *Phys. Rev. Lett.* **104**, 243001 (2010).
- [43] P. V. Demekhin, I. D. Petrov, V. L. Sukhorukov, W. Kielich, A. Knie, H. Schmoranzner, and A. Ehresmann, *J. Phys. B: At., Mol. Opt. Phys.* **43**, 165103 (2010).
- [44] H. Sann, C. Schober, A. Mhamdi, F. Trinter, C. Müller, S. K. Semenov, M. Stener, M. Waitz, T. Bauer, R. Wallauer *et al.*, *Phys. Rev. Lett.* **117**, 263001 (2016).
- [45] V. Averbukh and L. S. Cederbaum, *J. Chem. Phys.* **125**, 094107 (2006).
- [46] S. Kopelke, K. Gokhberg, L. S. Cederbaum, and V. Averbukh, *J. Chem. Phys.* **130**, 144103 (2009).
- [47] V. L. Jacobs and P. G. Burke, *J. Phys. B: At. Mol. Phys.* **5**, L67 (1972).
- [48] S. Salomonson, S. L. Carter, and H. P. Kelly, *Phys. Rev. A* **39**, 5111 (1989).
- [49] D. W. Lindle, T. A. Ferrett, U. Becker, P. H. Kobrin, C. M. Truesdale, H. G. Kerkhoff, and D. A. Shirley, *Phys. Rev. A* **31**, 714 (1985).
- [50] T. Havermeier, Photoionisation von Heliumdimeren, Ph.D. thesis, J. W. Goethe-Universität, Frankfurt am Main, 2010, [https://www.atom.uni-frankfurt.de/publications/files/Tilo\\_Havermeier\\_2010.pdf](https://www.atom.uni-frankfurt.de/publications/files/Tilo_Havermeier_2010.pdf).